Journal of Vibration Engineering & Technologies (2024) 12:2279–2293
https://doi.org/10.1007/s42417-023-00979-5

ORIGINAL PAPER

Optimum Design of Tuned Mass Dampers for Structures with Torsional Irregularity via Jaya Algorithm

Apaer Mubuli[1] · Sinan Melih Nigdeli[1] · Gebrail Bekdaş[1]

Received: 11 October 2022 / Revised: 3 February 2023 / Accepted: 12 April 2023 / Published online: 23 April 2023

Abstract

Background In this study, a tuned mass damper (TMD) was implemented on 3D irregular structures to reduce structural responses including the increased displacements of structures at corners due to torsional rotation.

Method A novel metaheuristic-based optimization methodology is presented for obtaining the optimum design of TMD. The methodology employs a metaheuristic algorithm called Jaya Algorithm and the codes of this algorithm were combined with dynamic analysis of TMD-included. To reduce torsional effects, the position of TMD on the plan is also a design variable additional to TMD parameters.

Results The method is tested on a single-story irregular structure as a theoretical study. Then, the application feasibility of the method was proved via a ten-story real-size structure. The optimum TMD is effective to reduce the maximum displacement by 25.71 and 22.69% for the single-story and ten-story structures, respectively.

Keywords Tuned mass dampers · Metaheuristic algorithms · Optimization · Control · Torsional irregularity · Earthquake

Introduction

The vibration control of structures under earthquake is considered to be a very important part of earthquake engineering and structural seismic design problem. Structural vibration control methods are classified into passive, active and semi-active and hybrid control. Among these control methods, the tuned mass damper system (TMD) is a passive control system and is one of the simplest and most reliable control devices. It consists of additional sub-structures on the main structure, which contains a mass, damping and spring stiffness generally. Its working principle is that when the structure under the action of a strong earthquake or a strong wind began to vibration, the frequency of the damper has been adjusted near to a certain structure frequency (usually the first natural frequency), so when the frequency is inspired, damper resonance occurs with interphase structure movement, energy distribution can be the effect on the structure of damping force. To obtain the most efficient energy dissipation capacity of the TMD, it is very important to determine the optimum parameters (i.e. the optimum tuning frequency ratio and optimum damping ratio) and the effectiveness of a TMD to control structural oscillations caused by different types of excitations is now well established.

The determination of the optimal parameters of TMD started after Frahm first invented the concept of using tuned mass dampers for vibration control in 1901. Den Hartog [1] considered the optimum design parameters for the first time for the undamped single degree of freedom (SDOF) system under harmonic load. Brock [2] and Den Hartog [1] describe the determination of the optimum parameters of the TMD for an undamped structure exposed to harmonic external excitation over a wide band of excitation frequencies. Based on Den Hartog's method, then Warburton and Ayorinde [3] obtained the optimal TMD parameters for the undamped structure under harmonic support excitement, where the acceleration amplitude is defined to be constant for all entry frequencies and other types of harmonic excitation. Explicit formulas for optimal parameters and the efficiency of a TMD to control structural oscillations due to different types of external excitations are now well established [4–11].

✉ Sinan Melih Nigdeli
melihnig@iuc.edu.tr

Apaer Mubuli
idikut_yildiz@hotmail.com

Gebrail Bekdaş
bekdas@iuc.edu.tr

[1] Department of Civil Engineering, Istanbul University-Cerrahpaşa, 34320, Avcilar, Istanbul, Turkey

The optimum tuning of TMDs is essential to make a feasible control of structure. In addition to that, the optimum TMD must be stable to the frequency deviation of the structure and adaptive and semi-active [12–15] types are useful in frequency deviation. Soil structure interaction is one of the reasons for frequency deviation [16]. Torsional irregularity is one of the factors that may change the optimum parameters that are found for a regular structure.

TMDs have been positioned on tall structures in all areas of the World since these are protective systems against the wind in addition to earthquakes in seismic zones. Examples include different types of mass dampers such as self-adjustable variable pendulum TMD [17], adaptive-passive eddy current pendulum TMD [18] and two-dimensional air spring based semi-active TMD for wind-induced vibration protection [19]. Studies on the application of TMDs to asymmetric structures subjected to seismic motion are relatively recent. A parametric study was carried out by Jangid and Datta [20] to study the efficiency of MTMDs to reduce the response of a simple torsionally coupled system of two degrees of freedom. Lin et al. [21] have demonstrated practical evaluations and vibration control effectiveness of passive tuned mass dampers (TMDs) using different optimization criteria for calculating the design parameters of MTMDs for irregular buildings modeled as multi-story torsional shear buildings under bidirectional random excitation. Lin and Wang studied the applicability of multiple tuned mass dampers (MTMD) on the vibration control of irregular buildings modeled as torsional-coupled structures due to base motions, considering the soil-structure interaction (SSI) effect [22]. Ueng et al. [23] using a similar model earlier in their work, determined the optimal parameters of the TMD system by minimizing the mean square displacement response ratio of the controlled degrees of freedom between the building with and without TMD. In addition, some practical design issues such as optimal location for installation, direction of movement and TMD numbers are explored in this work. Lin et al. [24] offer adjustable bidirectional shock absorbers (BiCTMDs) for monitoring the seismic response of buildings with an elastic asymmetric bidirectional plane. Almazán et al. [25] were investigated the response of asymmetric linear and nonlinear structures exposed to unidirectional and bidirectional seismic excitation, equipped with one or two Tuned Mass Dampers (TMD) whose parameter values are optimized by applying the general torsional balance concept. Taha et al. [26] investigated the effectiveness of torsion-tuned mass dampers (T-TMDs) in response control of asymmetrical buildings under bidirectional earthquake ground excitations. Akyurek et al. [27] proposed a newly developed Integrated Control System (ICS) to improve the safety and performance of torsionally irregular buildings with the effectiveness of TMD applied to the bidirectional eccentric Benchmark nine-story torsional irregular steel building constructed for the SAC steel project in California. Raze et al. [28] proposed a nonlinear digital vibration absorber that is connected to the structure with piezoelectric patches. Bukhari and Barry [29] controlled the nonlinear vibration of a beam by a nonlinear vibration absorber (NVA) that uses the exact natural frequencies and mode shapes of the beam. Zhao et al. [30] conducted dynamic analysis of a beam structure including nonlinear energy sink (NES) and various supports. A tuned nonlinear spring-inerter-damper vibration absorber was studied in the reduction of dynamic beam motions by Qian and Zou [31]. Zhao et al. [32] developed a method using multiple NES for vibration suppression of generally restrained pre-pressure beams.

Deciding optimal values of TMD parameters is a challenging task for structural engineers. Many researchers use different optimization algorithms. In the optimum design of the TMDs, two main ways can be chosen. In several studies, simplified formulations were proposed. These formulations were found for a single degree of freedom main system, but the formulation can be used by considering the critical vibration mode only. In these formulations, a frequency ratio

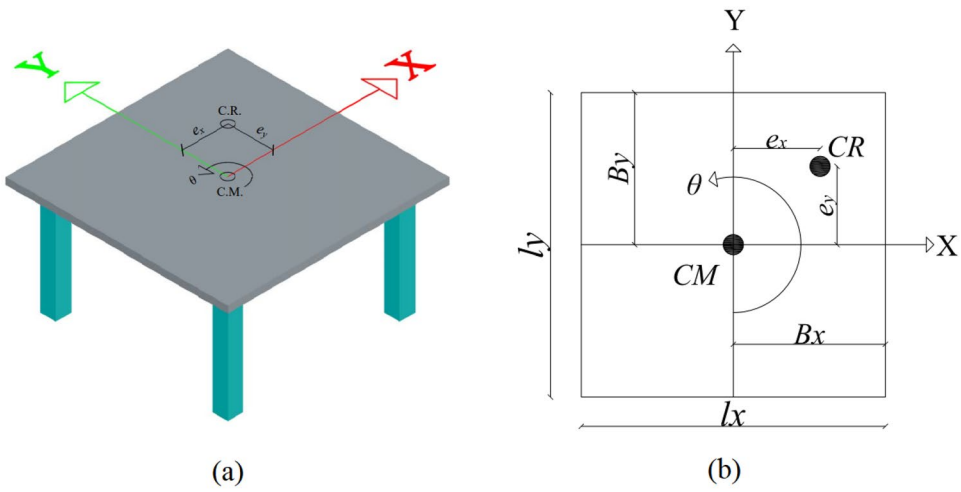

Fig. 1 **a** 3D view of the single-story building, **b** Plan view of the single-story building.

of TMD and structure (f_{opt}) and optimum TMD damping ratio ($\xi_{d,opt}$) are proposed. These formulations were derived by theoretical formulations by making some assumptions [1–3] or by using metaheuristic algorithms such as Particle Swarm Optimization [33] and Artificial Neural Network [34]. The second way is to couple a dynamic analysis code or software within the optimization process code. In optimization of TMDs, the most popular approaches are based on metaheuristic algorithms, and the algorithms such as Genetic Algorithm [35, 36], Particle Swarm Optimization [33, 37], Harmony Search [38, 39], Bat Algorithm [40, 41], Ant Colony Optimization [42], Flower Pollination Algorithm [43], Teaching Learning-Based Optimization and Jaya Algorithm (JA) [44] have been employed.

JA has been effectively employed in several structural engineering problems. For example, JA was employed in seismic design of planar and spatial steel frames [45], multi-objective optimum design of reinforced concrete (RC) structures [46], energy-based analysis of nonlinear plane-stress systems [48], design of 3D RC structures [48], optimum design of RC retaining walls [49] and optimization of prestressed steel trusses [50]. Also, JA was perfectly applied to structural control applications such as TMD [44], tuned liquid column damper [51], active tendon control [52] and active tuned mass dampers [53]. Due to previous usage in control systems and easy implementation of the single-phase JA, it was chosen as the optimization algorithm in the methodology.

Generally, TMDs are optimized for planer structures. This study is unique in the optimization of parameters in both directions considering the location of TMD in the plan to avoid torsional effects. For structures with torsional irregularity, the mode in the torsional rotation direction is related to the modes in two lateral directions. Due to that, the TMD tuning range for a 3D irregular building may be very than the mode frequency. Additionally, optimum positioning can be also considered as a design variable in the plan of the structure. In that case, a specific optimization approach is in need. In the present study, a novel optimization approach is proposed for 3D structures that have different properties in x and y directions to find the optimum parameters and placement of TMD positioned on the top of the structure. In addition to the theoretical single-story structure, the method was also applied to a real-size 10-story irregular structure.

Equation of Motion of 3D Building with TMD

In the study, the equations of motion are given for a single-story structure. It is known that the single-story torsion irregular structure has three degrees of freedom under the action of earthquakes in the x and y directions: lateral displacement in the x and y directions and rotational displacement (Fig. 1).

The center of mass is CM and the center of stiffness is shown as CR. The distances between the center of mass and the center of stiffness are shown with e_x and e_y as eccentricities in the x and y directions. Bx and By are distances expressing the location of the center of mass. lx and ly are the lengths of the structure in the x and y directions.

The structure has different stiffness values in x and y directions shown as k_x and k_y, respectively. The mass of structure is shown as m. The employed TMD on the top of the structure has mass (m_d), stiffness (k_{dx} and k_{dy} in x and y directions, respectively) and damping coefficients (c_{dx} and c_{dy} in x and y directions, respectively). TMD is positioned on the coordinates (a_x, a_y) to prevent torsional effects.

The equation of motion of the system with a TMD under earthquake excitation is:

$$M_{TMD}\ddot{x}_{TMD}(t) + C_{TMD}\dot{x}_{TMD}(t) + K_{TMD}x_{TMD}(t) = E_{TMD}\ddot{z}_g(t). \tag{1}$$

M_{TMD} represents the mass matrix of the system with TMD as shown in Eq. (2). M represent the mass matrix of 3D building without TMD as given in Eq. (3) including parameters of mass (m) and mass moment of inertia (J_0) of the structure story. J_0 is formulated as Eq. (4) where r is the radius of gyration. M_T is shown as Eq. (5) where m_d is the mass of TMD.

$$M_{TMD} = \begin{bmatrix} M & [0]_{3x2} \\ [0]_{2x3} & M_T \end{bmatrix} \tag{2}$$

$$M = \begin{bmatrix} m & 0 & 0 \\ 0 & m & 0 \\ 0 & 0 & J_0 \end{bmatrix} \tag{3}$$

$$J_0 = mr^2 \tag{4}$$

$$M_T = \begin{bmatrix} m_d & 0 \\ 0 & m_d \end{bmatrix}. \tag{5}$$

x_{TMD} represents the response vector and it is included in Eq. (1) with its derivatives respect to time shown with dots on it. As seen in Eq. (6), $x_{TMD}(t)$ can be written with structural responses; ux, uy and $u\theta$) for displacement in x and y directions and rotation on xy plane, respectively, and TMD responses including displacement in two directions (x_{dx}, x_{dy}).

$$x_{TMD}(t) = \begin{bmatrix} [u_x\, u_y u_\theta]^T \\ [x_{dx}\ \ x_{dy}]^T \end{bmatrix}. \tag{6}$$

K_{TMD} is the stiffness matrix of the combined system of structure and TMD (Eq. (7)) which includes K (Eq. (8)) that is the stiffness matrix of the structure without TMD and K_T given as Eq. (9).

$$K_{TMD} = \begin{bmatrix} K & [0] \\ [0]_{2\times3} & [0] \end{bmatrix} + K_T \tag{7}$$

$$K = \begin{bmatrix} k_x & 0 & -k_x e_y \\ 0 & k_y & k_y e_x \\ -k_x e_y & k_y e_x & k_0 + k_x e_y^2 + k_y e_x^2 \end{bmatrix} \tag{8}$$

$$K_T = \begin{bmatrix} k_{dx} & 0 & k_{dx}a_y & -k_{dx} & 0 \\ 0 & k_{dy} & k_{dy}a_x & 0 & -k_{dy} \\ k_{dx}a_y & k_{dy}a_x & k_{dx}a_y^2 + k_{dy}a_x^2 & -k_{dx}a_y & -k_{dy}a_x \\ -k_{dx} & 0 & -k_{dx}a_y & k_{dx} & 0 \\ 0 & -k_{dy} & -k_{dy}a_x & 0 & k_{dy} \end{bmatrix}. \tag{9}$$

C_{TMD} is the damping matrix of the structure with TMD as given Eq. (10).

$$C_{TMD} = \begin{bmatrix} C & [0]_{3\times2} \\ [0]_{2\times3} & [0]_{2\times2} \end{bmatrix} + C_T$$

$$C_{TMD} = \begin{bmatrix} C & [0]_{3\times2} \\ [0]_{2\times3} & [0]_{2\times2} \end{bmatrix} + C_T. \tag{10}$$

C is the damping matrix of structure without TMD and it can be found via Rayleigh damping which is proportional to M and K matrices as seen in Eq. (11). α and β coefficients can be found by using the damping ratios of first two modes. C_T is formulated as Eq. (12).

$$C = \alpha M + \beta K \tag{11}$$

$$C_T = \begin{bmatrix} c_{dx} & 0 & c_{dx}a_y & -c_{dx} & 0 \\ 0 & c_{dy} & c_{dy}a_x & 0 & -c_{dy} \\ c_{dx}a_y & c_{dy}a_x & c_{dx}a_y^2 + c_{dy}a_x^2 & -c_{dx}a_y & -c_{dy}a_x \\ -c_{dx} & 0 & -c_{dx}a_y & c_{dx} & 0 \\ 0 & -c_{dy} & -c_{dy}a_x & 0 & c_{dy} \end{bmatrix}. \tag{12}$$

The influence matrix of ground excitation (E_{TMD}) is given as Eq. (13). $\ddot{Z}(t)$ is the excitation vector (Eq. 14) that includes ground acceleration; $\ddot{x}_g(t)$ and $\ddot{y}_g(t)$ in x and y directions, respectively.

$$E_{TMD} = \begin{bmatrix} -m & 0 \\ 0 & -m \\ 0 & 0 \\ -m_d & 0 \\ 0 & -m_d \end{bmatrix} \tag{13}$$

$$\ddot{z}_g(t) = \begin{bmatrix} \ddot{x}_g(t) \\ \ddot{y}_g(t) \end{bmatrix}. \tag{14}$$

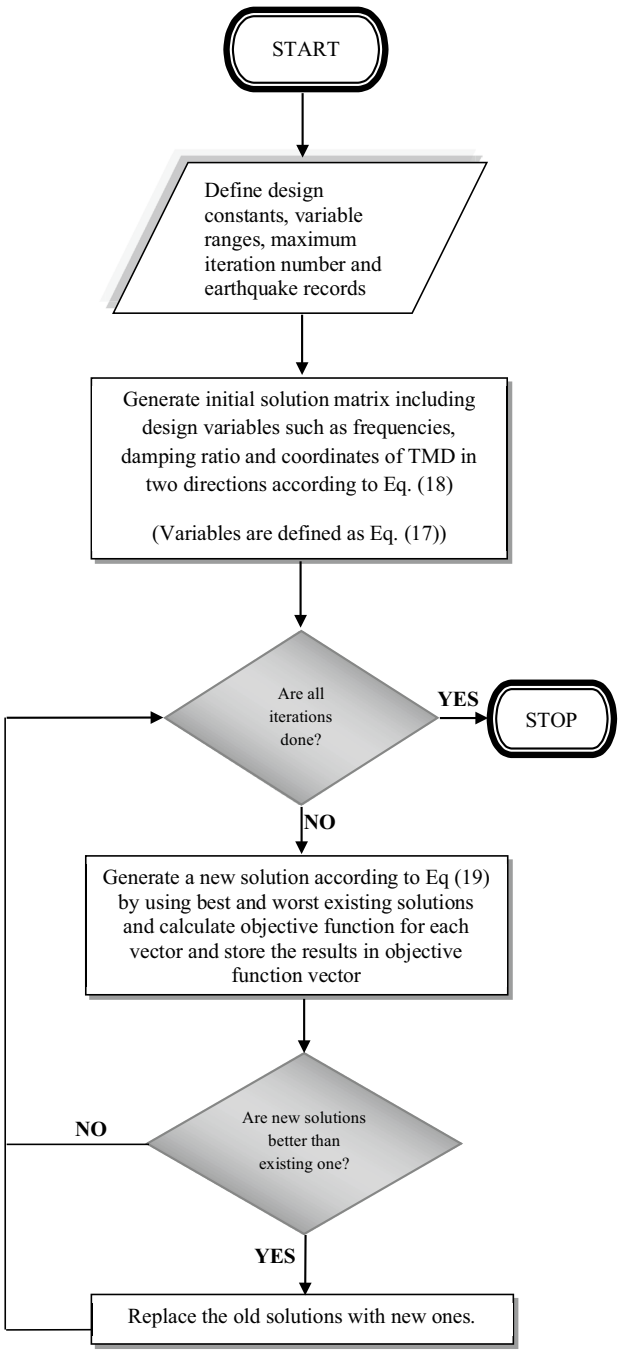

Fig. 2 Flowchart of JA

The Optimization Process

In the optimization process, the objective is to minimize the maximum displacement that occurs at the edge of the structures due to torsional irregularity under earthquake excitation. The optimized TMD parameters for irregular 3D structure are frequency in two directions (wdx and wdy) (Eq. 15), damping ratio in two directions (ξdx and ξdy) (Eq. 16) and

Table 1 FEMA earthquake records used in optimization [55]

No	Earthquake	Station	Year	Magnitude	FN component	FP component
1	Northridge	Beverly Hills—Mulhol	1994	6.7	NORTHR/MUL009	NORTHR/MUL279
2	Northridge	Canyon Country-WLC	1994	6.7	NORTHR/LOS000	NORTHR/LOS270
3	Duzce, Turkey	Bolu	1999	7.1	DUZCE/BOL000	DUZCE/BOL090
4	Hector Mine	Hector	1999	7.1	HECTOR/HEC000	HECTOR/HEC090
5	Imperial Valley	Delta	1979	6.5	IMPVALL/H-DLT262	IMPVALL/H-DLT352
6	Imperial Valley	El Centro Array #11	1979	6.5	IMPVALL/H-E11140	IMPVALL/H-E11230
7	Kobe, Japan	Nishi-Akashi	1995	6.9	KOBE/NIS000	KOBE/NIS090
8	Kobe, Japan	Shin-Osaka	1995	6.9	KOBE/SHI000	KOBE/SHI090
9	Kocaeli, Turkey	Duzce	1999	7.5	KOCAELI/DZC180	KOCAELI/DZC270
10	Kocaeli, Turkey	Arcelik	1999	7.5	KOCAELI/ARC000	KOCAELI/ARC090
11	Landers	Yermo fire station	1992	7.3	LANDERS/YER270	LANDERS/YER360
12	Landers	Coolwater	1992	7.3	LANDERS/CLW-LN	LANDERS/CLW-TR
13	Loma Prieta	Capitola	1989	6.9	LOMAP/CAP000	LOMAP/CAP090
14	Loma Prieta	Gilroy Array #3	1989	6.9	LOMAP/G03000	LOMAP/G03090
15	Manjil, Iran	Abbar	1990	7.4	MANJIL/ABBAR–L	MANJIL/ABBAR–T
16	Superstition Hills	El centro imp. Co	1987	6.5	SUPERST/B-ICC000	SUPERST/B-ICC090
17	Superstition Hills	Poe road (temp)	1987	6.5	SUPERST/B-POE270	SUPERST/B-POE360
18	Cape Mendocino	Rio dell overpass	1992	7.0	CAPEMEND/RIO270	CAPEMEND/RIO360
19	Chi-Chi, Taiwan	CHY101	1999	7.6	CHICHI/CHY101-E	CHICHI/CHY101-N
20	Chi-Chi, Taiwan	TCU045	1999	7.6	CHICHI/TCU045-E	CHICHI/TCU045-N
21	San Fernando	LA—hollywood stor	1971	6.6	SFERN/PEL090	SFERN/PEL180
22	Friuli, Italy	Tolmezzo	1976	6.5	FRIULI/A-TMZ000	FRIULI/A-TMZ270

Table 2 Characteristics of the single-story torsional irregularity structure [56]

Descriptions	Expression form and unit	Values
Mass	m (kg)	2923.5
The natural frequencies in the x, y, and θ directions	ω_x(Hz)	3.47
	ω_y(Hz)	3.81
	ω_θ(Hz)	4.16
Damping ratios in the x, y and θ directions	$\xi_x = \xi_y = \xi_\theta(\%)$	1.24
Center of gravity position	$B_x/r = B_y/r\ (m)$	$\sqrt{3/2}$
Rigidity center location	$e_x/r = e_y/r\ (m)$	0.3

location in two directions (ax and ay). The total number of design variables is six as listed in Eq. 17.

$$w_{dx} = \sqrt{\frac{k_{dx}}{m_d}},\ w_{dy} = \sqrt{\frac{k_{dy}}{m_d}} \tag{15}$$

$$\xi_{dx} = \frac{c_{dx}}{2m_d w_{dx}},\ \xi_{dy} = \frac{c_{dy}}{2m_d w_{dy}} \tag{16}$$

$$X_i = \begin{Bmatrix} w_{dx} \\ w_{dy} \\ \xi_{dx} \\ \xi_{dy} \\ a_x \\ a_y \end{Bmatrix}. \tag{17}$$

The optimization process uses Jaya Algorithm [54] which is a metaheuristic algorithm. In the process of numerical optimization using a metaheuristic algorithm, the design variable are assigned with candidate values within a defined solution range. This solution range must be suitable to physical conditions and logical values that may include possible optimum values in the range. As known, TMDs are tuned around the natural frequency of the structure.

Table 3 Optimum TMD parameters of the single-story structure

m_d(kg)	ω_{d_x}(rad/s)	ξ_{d_x}	ω_{d_y}(rad/s)	ξ_{d_y}	a_x (m)	a_y (m)
146.175	19.2652767	0.15265648	35.5463619	0.01001932	1.22470504	1.22422752

Table 4 The maximum displacement in the x-direction under 22 earthquake records for the single-story structure

Earthquake record No	Displacement in *x*-direction without TMD (m)	Displacement in *x*-direction with TMD (m)
1	0.022300175	0.016058242
2	0.022884199	0.013581704
3	0.038112968	0.028974505
4	0.011393793	0.010138460
5	0.014364185	0.008417161
6	0.031101029	0.019366877
7	0.029155743	0.022018147
8	0.008461972	0.006607591
9	0.018415678	0.013637725
10	0.003792635	0.003964214
11	0.011981953	0.010119119
12	0.020313335	0.016279714
13	0.032049446	0.023816721
14	0.020974038	0.018245954
15	0.025239099	0.017033254
16	0.014556829	0.011374383
17	0.014924041	0.012889370
18	0.025248974	0.015764644
19	0.016605699	0.010878853
20	0.024022089	0.020918041
21	0.012151268	0.010470923
22	0.015560022	0.015766907

At the first stage of the optimization process, the design constants are defined. The design constants include structural data, earthquake data and design variable ranges. In the optimization, multiple earthquake excitation were used and one with the maximum displacement was taken as the objective function, because TMD parameters must not specific to a single excitation and different TMD parameter configuration may show different performance under different ground acceleration records. As for the ranges of design variables, the location ranges are limited by the measures of controlled building. The damping ratios can be searched between 1 and 3%. The frequencies of TMD were searched between 0.8 times of natural frequency of the structure and 1.2 times of maximum frequency of the structure.

After the definition of constants, candidate design variables are generated within the range limits by using a random number between 0 and 1 (rand(1)) as seen in Eq. 18. Xi is the generated value for ith population. The initial solution matrix contains values of all populations.

$$X_i = X_{\min} + r\,and\,(1)\left(X_{\max} - X_{\min}\right). \tag{18}$$

The minimum and maximum ranges are denoted as Xmin and Xmax. After the definition of initial solutions, the candidate parameters are updated according to algorithm properties. The new solutions are accepted to store in the solution matrix if the objective function value is lower than the value of the existing set of design variables. For that reason, the dynamic analysis of the control system is done for all sets of earthquake excitations to find the value of the objective function.

To converge on the best optimum solution, several ideas have been proposed in the generation of a new candidate solution. Jaya Algorithm (JA) developed by Rao [54] is one of the basic metaheuristic algorithms that use a single phase in an iteration. In a single-phase, convergence is provided by using best (Xbest) and worst (Xworst) solutions together.

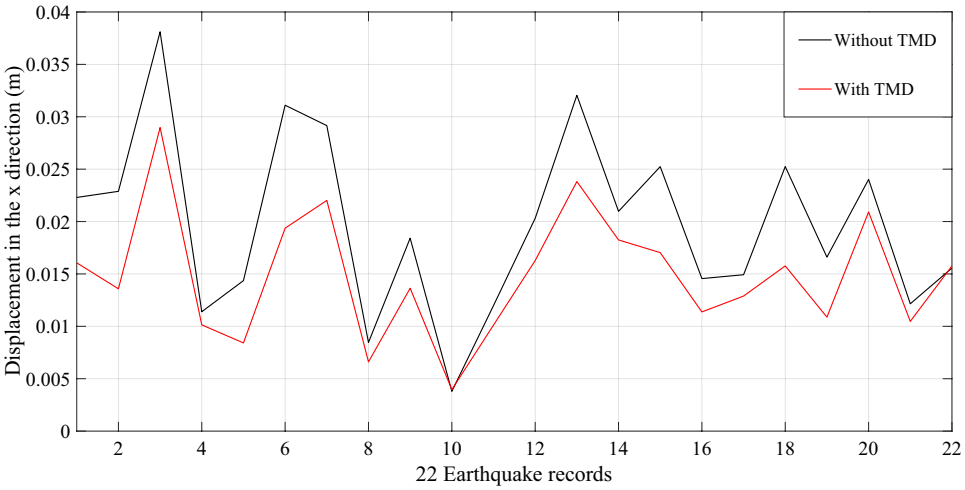

Fig. 3 The plot of maximum displacement in the x-direction under 22 earthquake records for the single-story structure

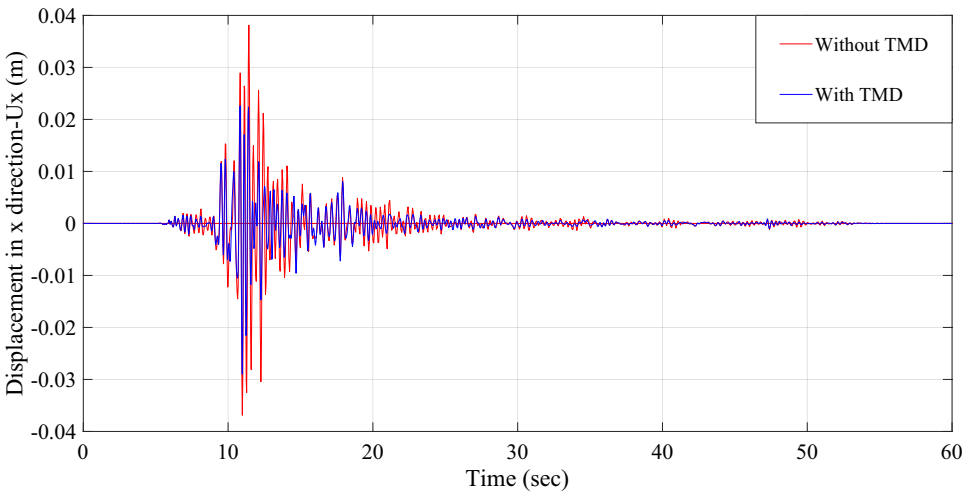

Fig. 4 The u_x displacement of the single-story structure according to the 3rd earthquake record

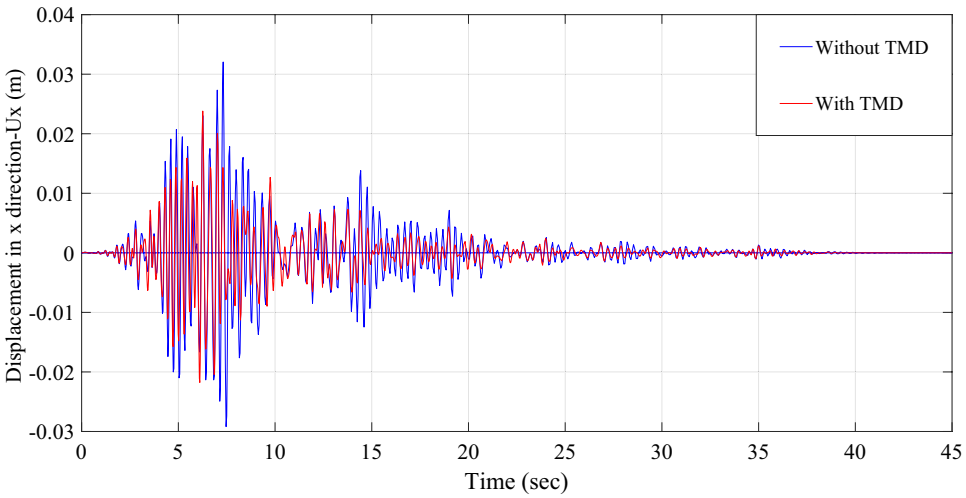

Fig. 5 The u_x displacement of the single-story structure according to the 13th earthquake record

For a new candidate solution of (t+1)th iteration (Xit+1), tth iteration values (Xit) are updated as Eq. (19).

$$X_i^{t+1} = X_i^t + rand(1)(X_{best} - |X_i^t|) - rand(1)(X_{worst} - |X_i^t|) \tag{19}$$

The iteration process was done for the maximum iteration number that is taken as 5000. In order prevent to trap of local optima, the population was taken as 10. Different from these parameters, JA has no specific parameters. This advantage makes JA simply one that is not needed to be configured for different algorithm parameters. The methodology is summarized in the flowchart given as Fig. 2.

Numerical Example

The method was applied for an optimum TMD that is positioned on a single-story irregular structural model and a real-size irregular 10 story structure. The mass ratio was considered as 5% for TMD. 22 far fault earthquake records given in Table 1 and defined in FEMA P-695 [55] were used in the optimization.

Single-Story Irregular Structure

The structural properties of the structure with torsional irregularity in question are given in Table 2.

Table 5 The maximum displacement in the y direction under 22 earthquake records for single-story structure

Earthquake record No	Displacement in *y* direction without TMD (m)	Displacement in *y* direction with TMD (m)
1	0.018062279	0.018380630
2	0.016824747	0.014626113
3	0.022206703	0.018763099
4	0.013769795	0.012369074
5	0.010371165	0.009906480
6	0.026750370	0.022996324
7	0.019433522	0.017727659
8	0.006555663	0.006561400
9	0.015846344	0.018018910
10	0.005153038	0.005531187
11	0.007553553	0.008563472
12	0.022994723	0.015966738
13	0.022230501	0.019304677
14	0.016021070	0.012398119
15	0.023851979	0.018755983
16	0.010000687	0.007374479
17	0.009782036	0.008644206
18	0.021359012	0.022815601
19	0.017175553	0.015494026
20	0.019117610	0.016509590
21	0.007116177	0.006580707
22	0.016326926	0.012701620

The optimum parameter values of TMD obtained from the optimization results with the JA are given in Table 3.

For the single-story structure, the maximum displacement at the x-direction occurs under the 3rd record in Table 1 which is the Bolu station records of the 1999 Düzce, Turkey earthquake. If the edge displacements affected by torsional rotation are considered, the maximum displacement is observed under the 13th record which is the Capitola record of the 1989 Loma Prieta, USA earthquake.

The maximum displacements in the x-direction are given for 22 records in Table 4 and plotted in Fig. 3 with a comparison of structure with and without TMD.

According to the critically selected earthquake record no. 3, the *x*-direction displacement of the structure plotted as Fig. 4 has a maximum of 0.03811 m in the case without TMD. In the structure with TMD, it is 0.02897 m. The efficiency of TMD for this excitation is 23.977%.

According to record no. 13, the efficiency of the TMD in the *x*-direction is 25.710%. In this case, the maximum u_x displacement is 0.03205 m without TMD and 0.02381 m with TMD as seen in Fig. 5.

The maximum displacements in y-direction are given in Table 5 and Fig. 6 shows the plot of these maximum displacements.

According to record no. 3, the maximum y-direction displacement of the structure is 0.02117 m in the case without TMD. In the case with TMD, it is 0.1876 m as seen in Fig. 7. The reduction effectiveness of TMD is 11.33%.

According to record no. 13, the maximum y-direction displacement of the single-story structure is 0.02223 m without TMD and 0.01930 m with TMD (Fig. 8). The effectiveness of TMD is 13.18%.

The maximum rotations are given in Table 6 and the maximums are plotted in Fig. 9. The maximum u_θ rotation of the

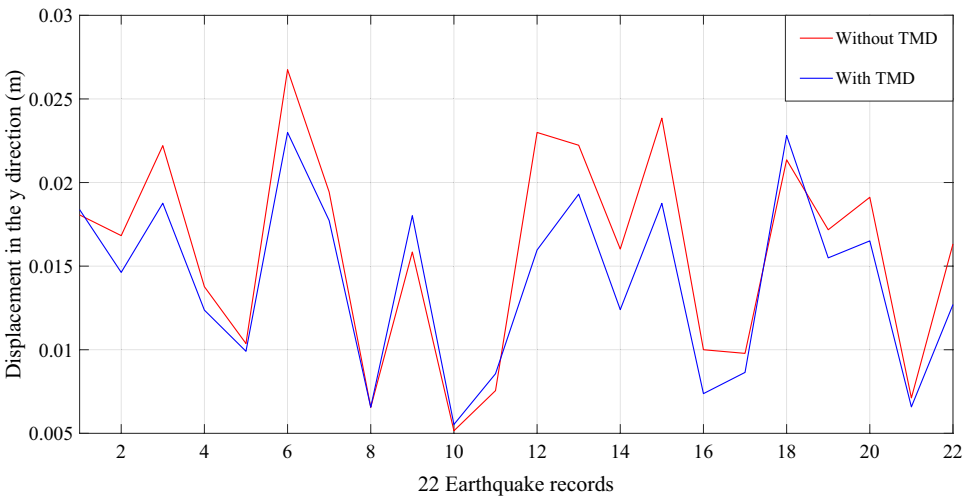

Fig. 6 The plot of maximum displacement in the y direction under 22 earthquake records for single-story structure

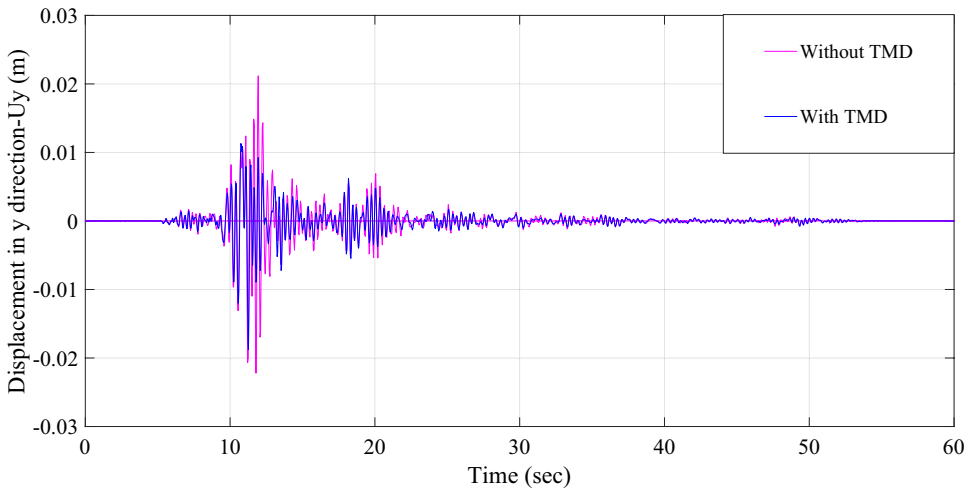

Fig. 7 The u_y displacement of the single-story structure according to the 3rd earthquake record

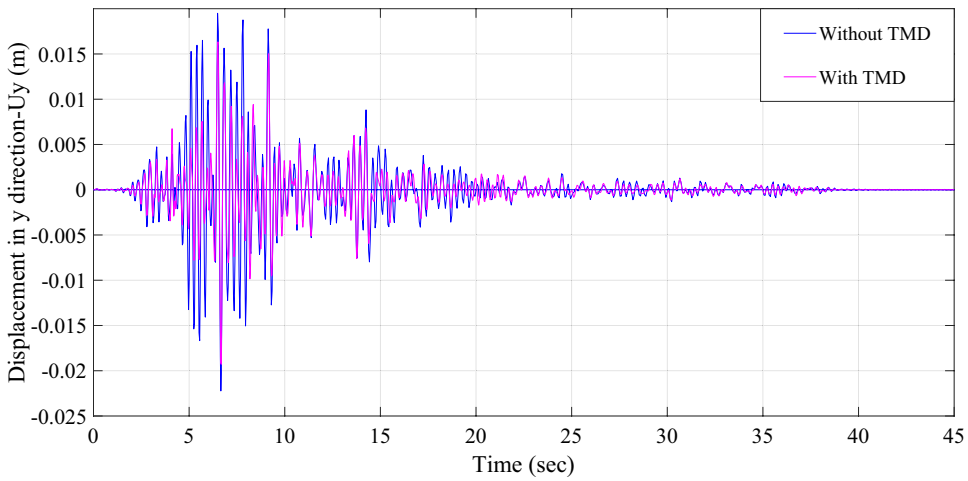

Fig. 8 The u_y displacement of the single-story structure according to the 13th earthquake record

structure with TMD in the θ direction is 0.01686 rad in the case without TMD, and 0.009467 rad in the case with TMD, in the analysis made according to the critically selected 3rd earthquake record. The effectiveness of TMD is 43.85%. According to record number 13, the maximum u_θ rotation of the structure with TMD in the θ direction is 0.01835 rad in the case without TMD and 0.013 rad in the case with TMD. The reduction effectiveness of TMD in u_θ rotation is 29.15%.

10-Story Irregular Structure

The method was applied to an asymmetrical ten-story frame-shear wall structure (Fig. 10) with equal floor height, equal floor mass, and equal floor mass radius of inertia. All slabs in the model were considered rigid diaphragms in the plan. Table 7 shows the properties of the materials and sections of the irregular ten-story frame-shear wall structure. The building height is 32 m and the total weight is 4849.831 tones.

The finite element model of the structure is modeled on the ETABS [57]. Table 8 shows the structure of the first three modal periods, modal participation mass ratio and modal direction factor values. Here, MPMR is the modal participant mass ratio (in the x, y and rz in torsional directions); MDF: refers to the modal direction factor (in the x, y and rz in torsional directions).

Structural properties of the main structure such as story mass, first three periods, the radius of story mass inertia and eccentricity required in the optimum design of the tuned

Table 6 The maximum displacement in the θ direction under 22 earthquake records for the single-story structure

Earthquake record No	Displacement in θ direction without TMD (rad)	Displacement in θ direction with TMD (rad)
1	0.011030975	0.007107148
2	0.014449166	0.006173394
3	0.016864264	0.009467439
4	0.005656977	0.005825205
5	0.006407108	0.006002410
6	0.012613624	0.009055438
7	0.013669264	0.011021468
8	0.003984197	0.002864669
9	0.007672297	0.005125547
10	0.003419237	0.002323366
11	0.005241648	0.003390187
12	0.015897600	0.009100361
13	0.018350580	0.012998686
14	0.014594521	0.008565537
15	0.016240213	0.011920778
16	0.007916350	0.004213145
17	0.007851297	0.004698565
18	0.015224585	0.010358687
19	0.007618713	0.006649226
20	0.013590661	0.011522640
21	0.005696050	0.003693415
22	0.010715127	0.006349864

mass dampers are given in Table 9. These parameter values were obtained with the ETABS structural analysis program.

Using the structural characteristics of the main structure from Table 9, optimization values of TMD obtained by using Jaya algorithm are given in Table 10.

IMPVALL/H-E11140 record in the *x*-direction and IMPVALL/H E11230 record in the *y*-direction of the El-Centro earthquake that occurred in 1979 were selected as the critical earthquake among a total of 44 earthquake records in *x* and *y* directions.

The results of the time history analysis with the ETABS package analysis program under these critical earthquake excitations are shown in the tables and figures below. Only the translation and rotation graphs under the selected critical earthquake record in the *x* and *y* directions of the 1923 nodal point in the 2-dimensional plan view in Fig. 9 are given in Figs. 11, 12, 13. The effectiveness of TMD at other nodes is given in Table 11.

From the results of Table 11, it is seen that the efficiency of TMD is more effective at the node 1923 than the other corner points in reducing the translations in the *x* and *y* directions and the rotations in the θ direction, under the influence of earthquake excitation. The optimum TMD is effective on x direction values since these values are bigger than the responses in the y-direction. In that case, the x-direction results are considered in the optimization objective. Also, the best effect of TMD was seen in the farthest point to the center of the floor.

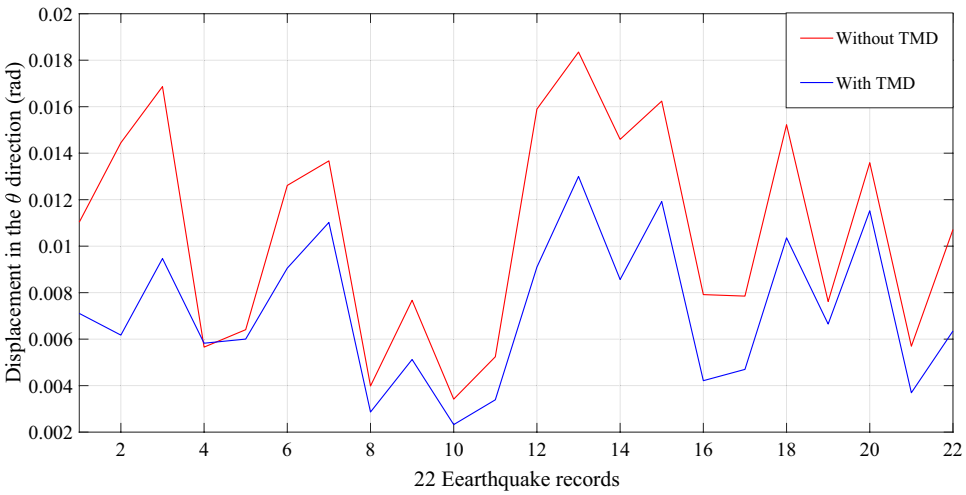

Fig. 9 The plot of maximum displacement in the θ direction under 22 earthquake records for single-story structure

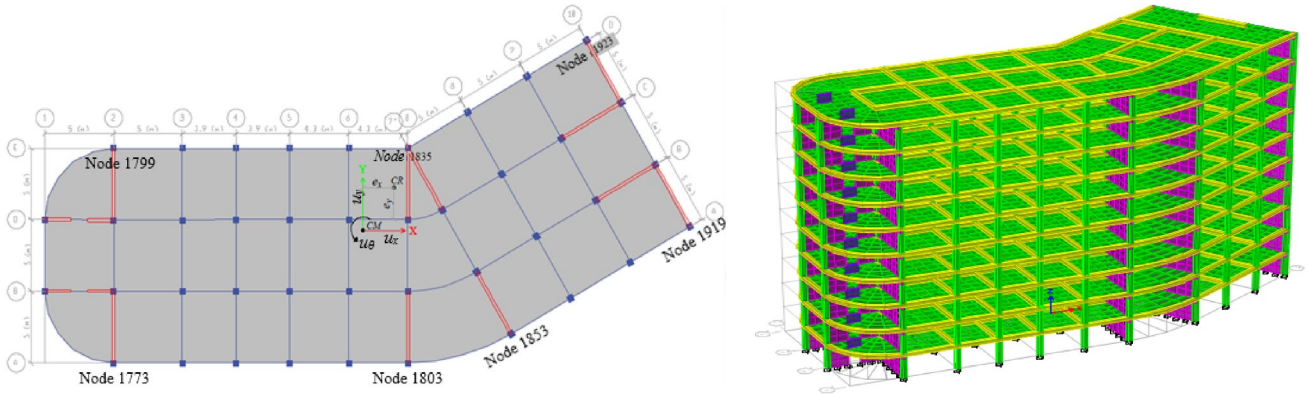

(a) 2D plan view (b) 3D view of the building

Fig. 10 10-story frame-Shear wall irregular structure **a** 2D plan view **b** 3D view of the building

Table 7 Material and section properties of the main structure

Material and section properties	
Type of building	Frame-shear wall structure
Number of floors	10
Floor height	3.2 m
Modulus of elasticity	32,000 Mpa
Poisson's ratio	0.2
Modal damping ratio	0.05
Column size	400×400 mm
Beam size	250×450 mm
Shear wall thickness	200 mm
Slab thickness	150 mm

Table 8 Dominant period of the ten-story building, MPMR and MDF values

Mode	1	2	3
Period (sec)	0.256	0.214	0.176
MPMRx	0.8036	0.0001	0.0447
MPMRy	0.0147	0.6064	0.2273
MPMRrz	0.0303	0.2432	0.5751
MDFx	0.947	0	0.053
MDFy	0.017	0.715	0.267
MDFrz	0.035	0.284	0.68

Table 9 Parameters of the main structure required for optimization

Story No	Floor mass *(kg)*	Floor mass radius of inertia r (m)	Eccentricity e_x (m)	Eccentricity e_y (m)
10	411,262.98	13.93914009	2.5049	2.6145
9	484,983.1	14.27583242	2.2301	2.478376
8	484,983.1	14.27583242	2.2301	2.478376
7	484,983.1	14.27583242	2.2301	2.478376
6	484,983.1	14.27583242	2.2301	2.478376
5	484,983.1	14.27583242	2.2301	2.478376
4	484,983.1	14.27583242	2.2301	2.478376
3	484,983.1	14.27583242	2.2301	2.478376
2	484,983.1	14.27583242	2.2301	2.478376
1	484,983.1	14.27583242	2.2301	2.478376

Table 10 Optimum parameter values of TMD

Descriptions	Parameters and unit	Parameters value
Mass	m_d (kg)	238,805.544
Natural frequency in the *x* and *y* directions	ω_{dx} (Hz)	26.97937597
	ω_{dy} (Hz)	34.03327077
Damping ratio in *x* and *y* directions	ξ_{dx}	0.078387203
	ξ_{dy}	0.099867359
Optimum position in the *x* and *y* directions	*x (m)*	10
	y (m)	10

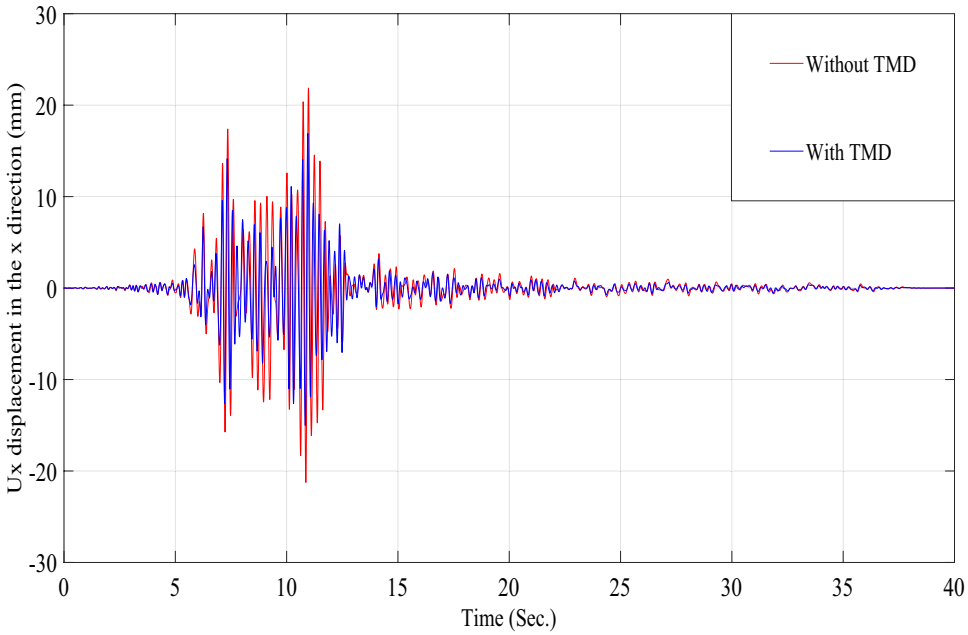

Fig. 11 u_x displacement under critical seismic excitation in *x*-direction at node 1923.

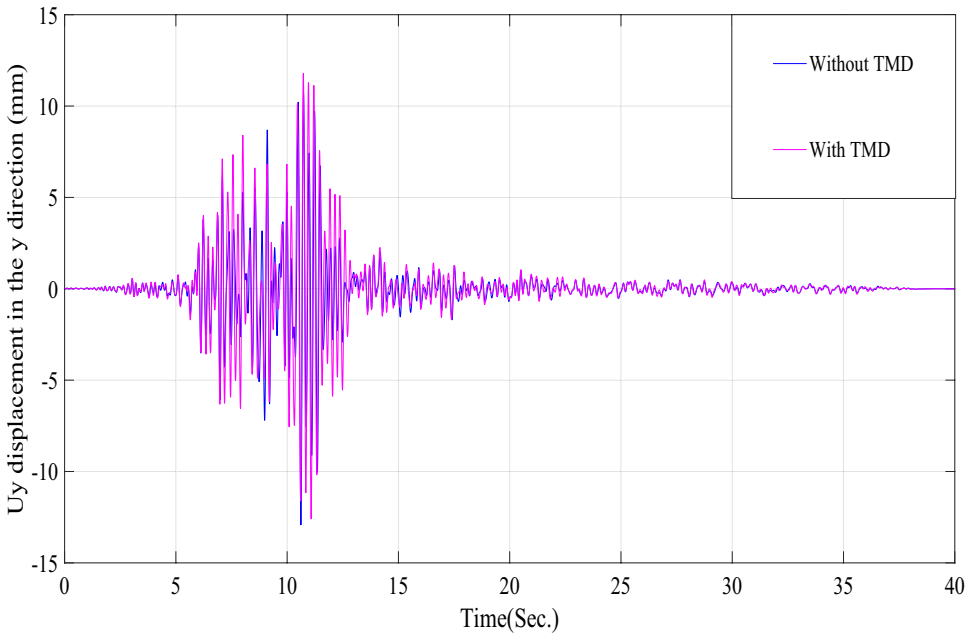

Fig. 12 u_y displacement under critical seismic excitation in *y*-direction at node 1923.

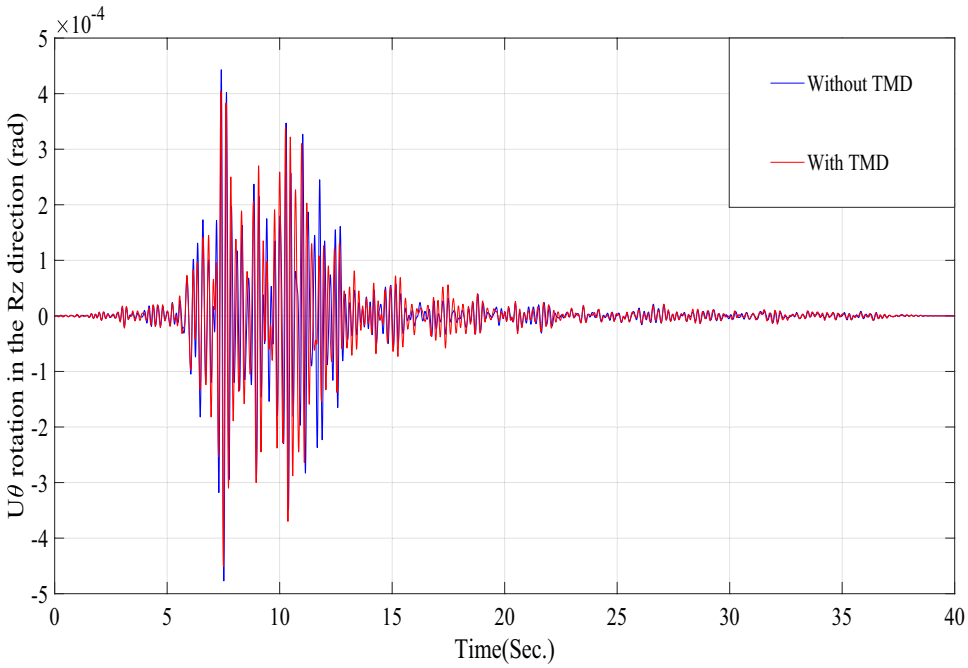

Fig. 13 u_θ rotation under critical seismic excitation in *y*-direction at node 1923.

Table 11 TMD efficiency of the four corners of the top floor

Node No	Parameters status of TMD	Response		
		u_x (mm)	u_y (mm)	u_θ (rad)
1773	Without TMD	25.686	14.93	0.000477
	With TMD	22.743	15.599	0.000451
	Effectiveness of TMD	11.46%	− 4.48%	5.45%
1799	Without TMD	22.946	14.93	0.000477
	With TMD	18.8	15.599	0.000451
	Effectiveness of TMD	18.07%	− 4.48%	5.45%
1919	Without TMD	23.844	14.114	0.000477
	With TMD	20.189	14.366	0.000451
	Effectiveness of TMD	15.33%	− 1.79%	5.45%
1923	Without TMD	21.866	12.918	0.000477
	With TMD	16.904	12.588	0.000451
	Effectiveness of TMD	22.69%	2.55%	5.45%

Conclusion

An optimization methodology for torsionally irregular structures with TMD was proposed to find optimum TMD properties and locations in the plan. The study was tested on a model single-story structure and a real structure with ten stories.

For the TMD positioned on the single-story structure, x-direction responses are more affected than the ones in the y-direction. As reported 25.71% reduction in the maximum displacement is provided for the single-story structure. Also, a 13.18% reduction is provided for maximum response in the y-direction. The essential effect of TMD is observed on maximum rotation by 43.85%.

The efficiency of the method was provided on a ten-story real-size structure with an 11.46% reduction for the maximum displacement. For the node affected by the most torsional irregularity, the reduction percentage is 22.69%. For y-direction responses, TMD is not so effective since the maximum responses in this direction are very low compared to x-direction responses.

In future work, multiple tuned mass dampers can be optimized for irregular 3D structures via the proposed methodology. Also, a multi-objective method can be provided to also obtain a reduction in the direction with less displacement.

Data availability Data is available on request to authors.

Declarations

Conflict of interest None of the authors have a conflict of interest to disclose.

References

1. Den Hartog JP (1956) Mechanical vibrations, 4th edn. McGraw-Hill, New York
2. Brock JE (1946) A note on the damped vibration absorber. J Appl Mech ASME 13:A-284
3. Warburton GB, Ayorinde EO (1980) Optimum absorber parameters for simple systems. Earthq Eng Struct Dyn 8:197–217

4. Ayorinde EO, Warburton GB (1980) Minimizing structural vibration with absorbers. Earthq Eng Struct Dyn 8:219–236
5. Warburton GB (1981) Optimum absorber parameters for minimizing vibration response. Earthq Eng Struct Dyn 9:251–262
6. Warburton GB (1982) Optimum absorber parameters for various combinations of response and excitation parameters. Earthq Eng Struct Dyn 10:381–401
7. Tsai HC, Lin GC (1993) Optimum tuned mass dampers for minimizing steadystate response of support excited and damped system. Earthq Eng Struct Dyn 22:957–973
8. Tsai HC, Lin GC (1993) Explicit formulae for optimum absorber parameters for force excited and viscously damped systems. J Sound Vib 89:385–396
9. Thompson AG (1981) Optimum tuning and damping of a dynamic vibration absorber applied to a force excited and damped primary system. J Sound Vib 77:403–415
10. Fujino Y, Abe M (1993) Design formulas for tuned mass dampers based on a perturbation technique. Earthq Eng Struct Dyn 22:833–854
11. Macinante JA (1984) Seismic mountings for vibration isolation. John Wiley and Sons, Inc., New York
12. Wang L, Shi W, Li X, Zhang Q, Zhou Y (2019) An adaptive-passive retuning device for a pendulum tuned mass damper considering mass uncertainty and optimum frequency. Struct Control Health Monit 26(7):e2377
13. Wang L, Shi W, Zhou Y, Zhang Q (2020) Semi-active eddy current pendulum tuned mass damper with variable frequency and damping. Smart Struct Syst 25(1):65–80
14. Wang L, Nagarajaiah S, Shi W, Zhou Y (2022) Seismic performance improvement of base-isolated structures using a semi-active tuned mass damper. Eng Struct 271:114963
15. Wang L, Nagarajaiah S, Shi W, Zhou Y (2021) Semi-active control of walking-induced vibrations in bridges using adaptive tuned mass damper considering human-structure-interaction. Eng Struct 244:112743
16. Wang L, Shi W, Zhou Y (2022) Adaptive-passive tuned mass damper for structural aseismic protection including soil–structure interaction. Soil Dyn Earthq Eng 158:107298
17. Wang L, Shi W, Zhou Y (2019) Study on self-adjustable variable pendulum tuned mass damper. Struct Design Tall Spec Build 28(1):e1561
18. Wang L, Nagarajaiah S, Shi W, Zhou Y (2020) Study on adaptive-passive eddy current pendulum tuned mass damper for wind-induced vibration control. Struct Design Tall Spec Build 29(15):e1793
19. Wang Y, Wang L, Shi W (2021) Two-dimensional air spring based semi-active TMD for vertical and lateral walking and wind-induced vibration control. Struct Eng Mech 80(4):377–390
20. Jangid RS, Datta TK (1997) Performance of multiple tuned mass dampers for torsionally coupled system. Earthq Eng Struct Dynam 26:307–317
21. Lin C, Ueng J, Huang T (1999) Seismic response reduction of irregular buildings using passive tuned mass dampers. Eng Struct 22:513–524
22. Lin CC, Wang JF (2005) Seismic performance of multiple tuned mass dampers for soil-irregular building interaction systems. Int J Solid Struct 42:5536–5554
23. Ueng J-M, Chi-Chang L, Wang J-F (2008) Practical design issues of tuned mass dampers for torsionally coupled building under earthquakes loadings. Struct Des Tall Spec Build 17:133–165
24. Lin JL, Tsai KCH, Yu YJ (2011) Bi-directional coupled tuned mass dampers for the seismic response control of two-way asymmetric-plan buildings. Earthquake Eng Struct Dynam 140:675–690
25. Almazan JL, Aguirre JJ, Espinoza G (2012) Torsional balance of asymmetric structures by means of tuned mass dampers. Eng Struct 42:308–328
26. Taha AE, Elias S, Matsagar V, Jain AK (2019) Seismic response control of asymmetric buildings using tuned mass dampers. Struct Design Tall Spec Build 28:e1673
27. Akyürek O, Suksawang N, Go HT (2019) Vibration control for torsionally irregular buildings by integrated control system. Eng Struct 201:109775
28. Raze G, Jadoul A, Guichaux S, Broun V, Kerschen G (2019) A digital nonlinear piezoelectric tuned vibration absorber. Smart Mater Struct 29(1):015007
29. Bukhari M, Barry O (2020) Exact nonlinear dynamic analysis of a beam with a nonlinear vibration absorber and with various boundary conditions. J Comput Nonlinear Dyn 15(1):011003
30. Zhao Y, Du J, Liu Y (2021) Vibration suppression and dynamic behavior analysis of an axially loaded beam with NES and nonlinear elastic supports. J Vibrat Cont 29(3–4):10775463211053456
31. Qian F, Zuo L (2021) Tuned nonlinear spring-inerter-damper vibration absorber for beam vibration reduction based on the exact nonlinear dynamics model. J Sound Vib 509:116246
32. Zhao Y, Du J, Chen Y, Liu Y (2022) Dynamic behavior and vibration suppression of a generally restrained pre-pressure beam structure attached with multiple nonlinear energy sinks. Acta Mech Solida Sinica 36(1):1–16
33. Leung AYT, Zhang H (2009) Particle swarm optimization of tuned mass dampers. Eng Struct 31(3):715–728
34. Yucel M, Bekdaş G, Nigdeli SM, Sevgen S (2019) Estimation of optimum tuned mass damper parameters via machine learning. J Build Eng 26:100847
35. Hadi MNS, Arfiadi Y (1998) Optimum design of absorber for MDOF structures. J Struct Eng-ASCE 124:12721280
36. Marano GC, Greco R, Chiaia B (2010) A comparison between dierent optimization criteria for tuned mass dampers design. J Sound Vibrat 329:4880–4890
37. Leung AYT, Zhang H, Cheng CC, Lee YY (2008) Particle swarm optimization of TMD by non-stationary base excitation during earthquake. Earthquake Eng Struct Dynam 37:1223–1246
38. Bekdaş G, Nigdeli SM (2011) Estimating optimum parameters of tuned mass dampers using harmony search. Eng Struct 33:2716–2723
39. Nigdeli SM, Bekdaş G (2017) Optimum tuned mass damper design in frequency domain for structures. KSCE J Civ Eng 21(3):912–922
40. Bekdaş G, Nigdeli SM (2017) Metaheuristic based optimization of tuned mass dampers under earthquake excitation by considering soil-structure interaction. Soil Dyn Earthq Eng 92:443–461
41. Bekdaş G, Nigdeli SM, Yang XS (2018) A novel bat algorithm based optimum tuning of mass dampers for improving the seismic safety of structures. Eng Struct 159:89–98
42. Farshidianfar A, Soheili S (2013) Ant colony optimization of tuned mass dampers for earthquake oscillations of high-rise structures including soil-structure interaction. Soil Dyn Earthquake Eng 51:14–22
43. Bekdaş G, Nigdeli SM, Yang X-S (2017) Metaheuristic Based Optimization for Tuned Mass Dampers Using Frequency Domain Responses. In: Harmony Search Algorithm. Advances in Intelligent Systems and Computing. Del Ser J (eds). 271–279. Springer
44. Bekdaş G, Kayabekir AE, Nigdeli SM, Toklu YC (2019) Tranfer function amplitude minimization for structures with tuned mass dampers considering soil-structure interaction. Soil Dyn Earthq Eng 116:552–562
45. Degertekin SO, Tutar H (2022) Optimized seismic design of planar and spatial steel frames using the hybrid learning based jaya algorithm. Adv Eng Softw 171:103172

46. Yücel M, Nigdeli SM, Bekdaş G (2022) June). Generation of sustainable models with multi-objective optimum design of reinforced concrete (RC) structures. In Struct 40:223–236
47. Toklu YC, Kayabekir AE, Bekdaş G, Nigdeli SM, Yücel M (2020) Analysis of plane-stress systems via total potential optimization method considering nonlinear behavior. J Struct Eng 146(11):04020249
48. Aslay SE, Dede T (2022) 3D cost optimization of 3 story RC constructional building using Jaya algorithm. Struct 40:803–811
49. Öztürk HT, Dede T, Türker E (2020) Optimum design of reinforced concrete counterfort retaining walls using TLBO Jaya algorithm. Struct 25:285–296
50. Aydın Z (2022) Size, layout and tendon profile optimization of prestressed steel trusses using Jaya algorithm. Struct 40:284–294
51. Ocak A, Bekdaş G, Nigdeli SM (2022) A metaheuristic-based optimum tuning approach for tuned liquid dampers for structures. Struct Design Tall Spec Build 31(3):e1907
52. Ulusoy S, Nigdeli SM, Bekdaş G (2021) Novel metaheuristic-based tuning of PID controllers for seismic structures and verification of robustness. J Build Eng 33:101647
53. Kayabekir AE, Nigdeli SM, Bekdaş G (2022) A hybrid metaheuristic method for optimization of active tuned mass dampers. Comput-Aided Civil Infrastruct Eng 37(8):1027–1043
54. Rao R (2016) Jaya: A simple and new optimization algorithm for solving constrained and unconstrained optimization problems. Int J Ind Eng Comput 7(1):19–34
55. FEMA P-695 (2009) Quantification of building seismic performance factors, Federal emergency management agency. Washington DC
56. Lin CC, Chang CC, Ve Wang J (2010) Active control of irregular buildings considering soil-structure interaction effects. Soil Dynam Earthquake Eng 30:98–109
57. CSI "ETABS Building Analysis and Design" Computers and Structures Inc. Berkeley, California.